Impact of Eurasian spring snow decrement on East Asian summer precipitation

Ruonan Zhang, Renhe Zhang*, Zhiyan Zuo

Chinese Academy of Meteorological Sciences, Beijing, China

In the present study, we investigated the relationship between Eurasian spring snow decrement (SSD) and East Asian summer precipitation and the related thermodynamic and dynamic mechanisms using both observational data and the CAM3.1 model. The results show that the second EOF mode of Eurasian SSD exhibits a west-east dipole pattern, with a negative center located over eastern Europe and the West Siberia Plain (EEWSP) and a positive center over the area around Baikal Lake (BL). This anomalous SSD pattern is significantly associated with the third EOF mode of East Asian summer rainfall through triggering an anomalous mid-latitude Eurasian wave train. The reduced SSD over EEWSP tends to decrease the local soil moisture from spring to the following summer, thereby increase the surface heat flux and near-surface temperatures. Similarly, the increase in SSD over BL is accompanied by anomalously low near-surface temperatures. Changes in near-surface temperatures further intensify the meridional temperature gradient and lower-level baroclinicity, leading to the acceleration of the upper-level subtropical westerly jet stream. At the 500 hPa geopotential heights, an anomalous cyclone and anomalous anticyclone emerge to the north and south, respectively, of the exit region of East Asian subtropical jet stream. Meanwhile, the changed surface thermal conditions enhance the local 1000–500 hPa thickness over EEWSP while decreasing it over BL. These factors both create favorable physical conditions for the maintenance and enhancement of the anomalous mid-latitude Eurasian wave train prevailing over the regions from eastern Europe eastward to the Northwest Pacific. We further explored the origin of the Eurasian wave train and found that there are zonally oriented WAFs spreading from eastern Europe eastward to East Asia. This finding demonstrates the role of anomalous SSD in triggering the Eurasian wave train. These circulation patterns ultimately significantly influence the precipitation over East Asia, especially over China, with excessive precipitation over regions west of BL, northeastern China and the Yellow River valley and deficient precipitation over Inner Mongolia and southern China. Therefore, Our study confirms the significant role of Eurasian SSD in influencing East Asian summer precipitation. Our model results demonstrate that the CAM3.1 can reproduce the positive summer precipitation anomalies over most of northern East Asia and negative anomalies over southern China. Corresponding to the imposed anomalous Eurasian SSD forcings in CAM3.1, positive surface air temperature and atmospheric thickness responses over EEWSP and negative responses over BL are primarily simulated. In the simulation the subtropical jet stream over East Asia is strengthened, the Eurasian mid-latitude wave train is formed, and reinforced WAFs propagate from eastern Europe to East Asia. These simulated dynamic and thermodynamic processes result in according precipitation anomalies to occur over East Asia.

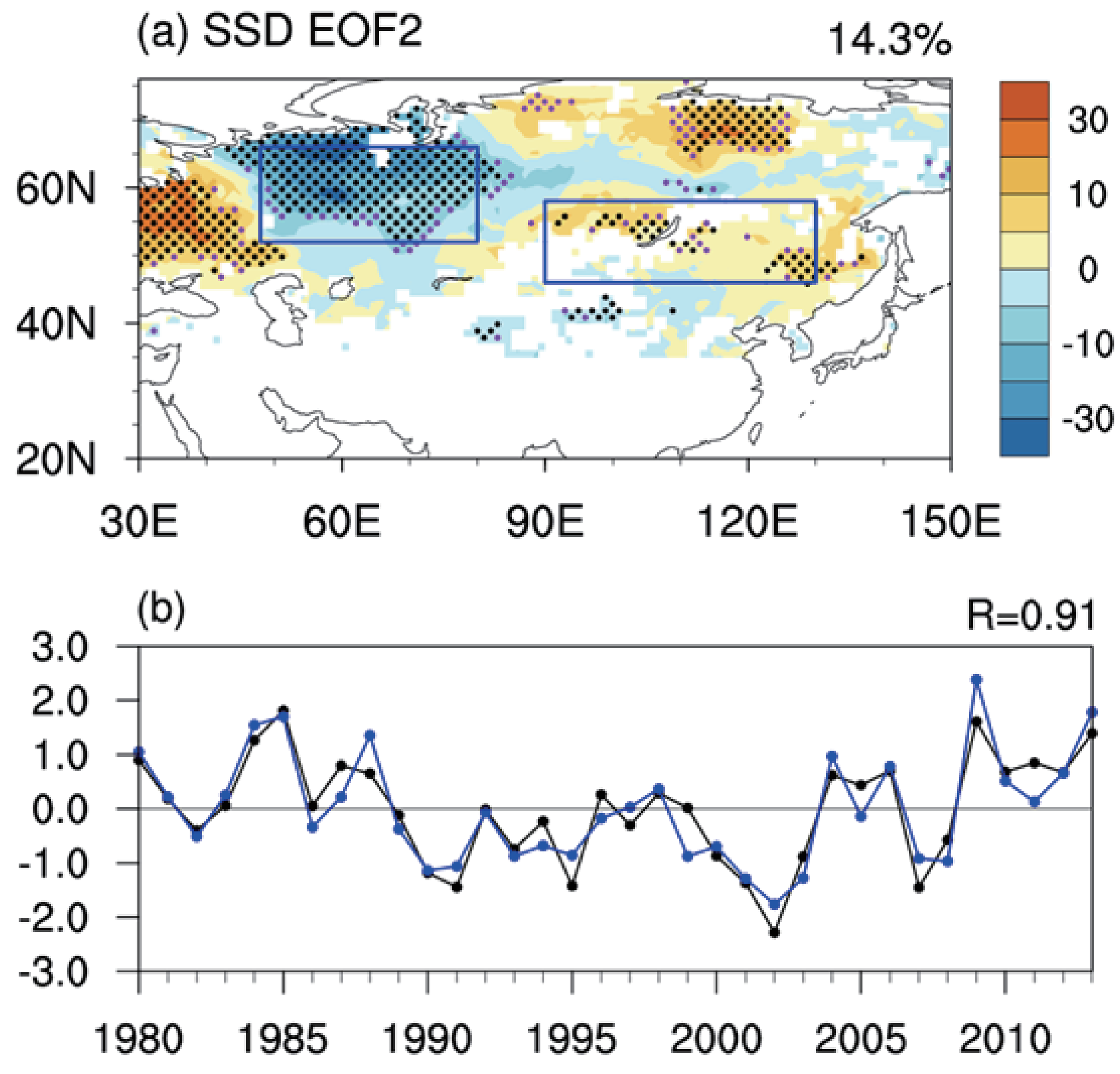

Figure 1. (a) Spatial pattern (shadings, units: mm) of the second EOF (EOF2) and (b) detrended time series of the second principal component (PC2, black line) of SSD over the Eurasian continent during 1980–2013. The blue line in (b) shows the SSDI index defined as the difference of SSD between the rectangles with positive values (46º–58ºN, 96º–138ºE) and negative values (54º–68ºN, 48º–84ºE) shown in (a). Purple and black dotted areas in (a) denote values with statistical significance exceeding the 90% and 95% confidence levels, respectively.

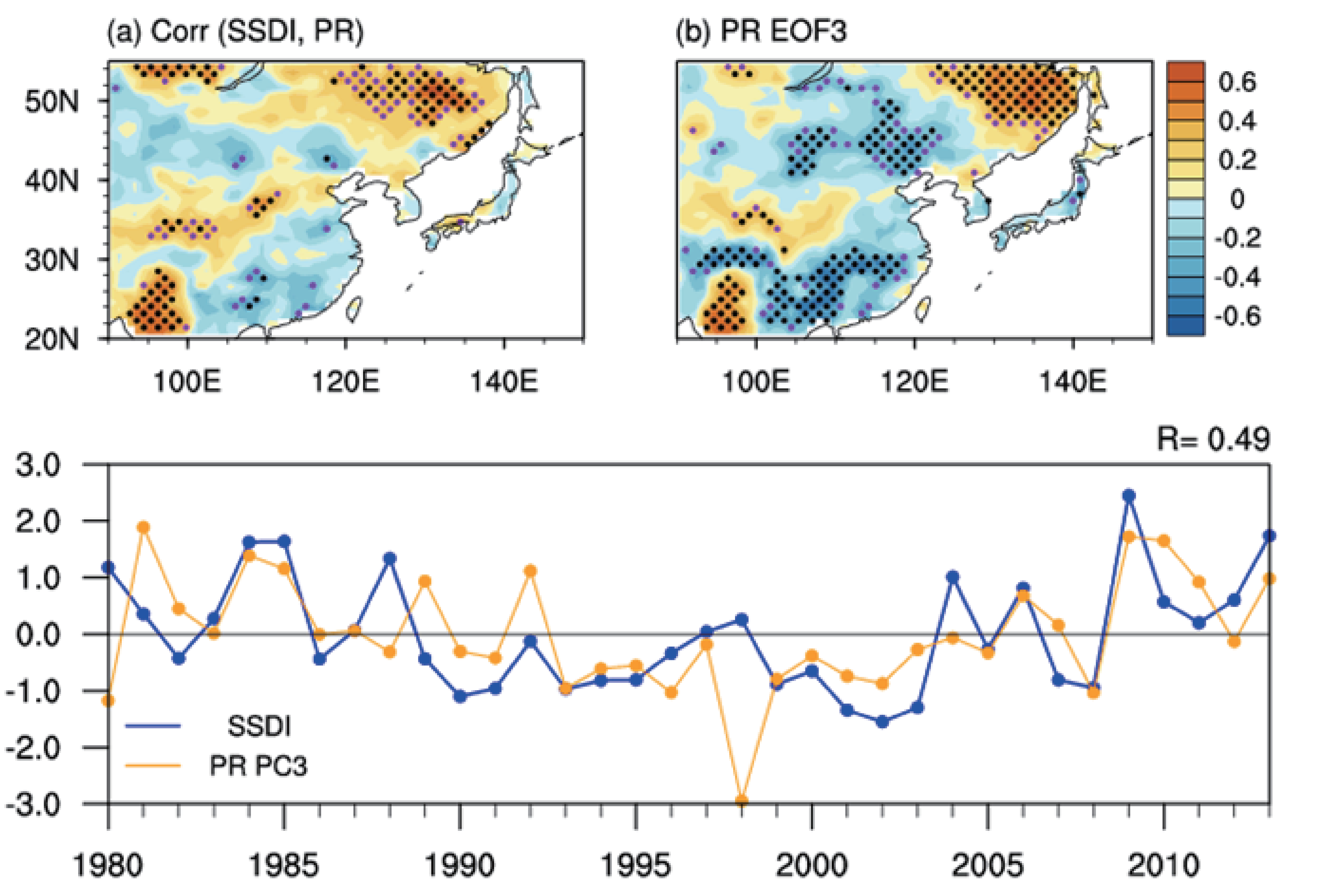

Figure 2 (a) Correlation coefficients between the SSDI index and the subsequent summer precipitation, (b) spatial pattern of the third EOF mode of East Asian summer precipitation, and (c) detrended time series of SSDI and summer precipitation (PC3). R represents the correlation coefficient between the two indices. Purple and black dotted areas denote values with statistical significance exceeding the 90% and 95% confidence levels, respectively.

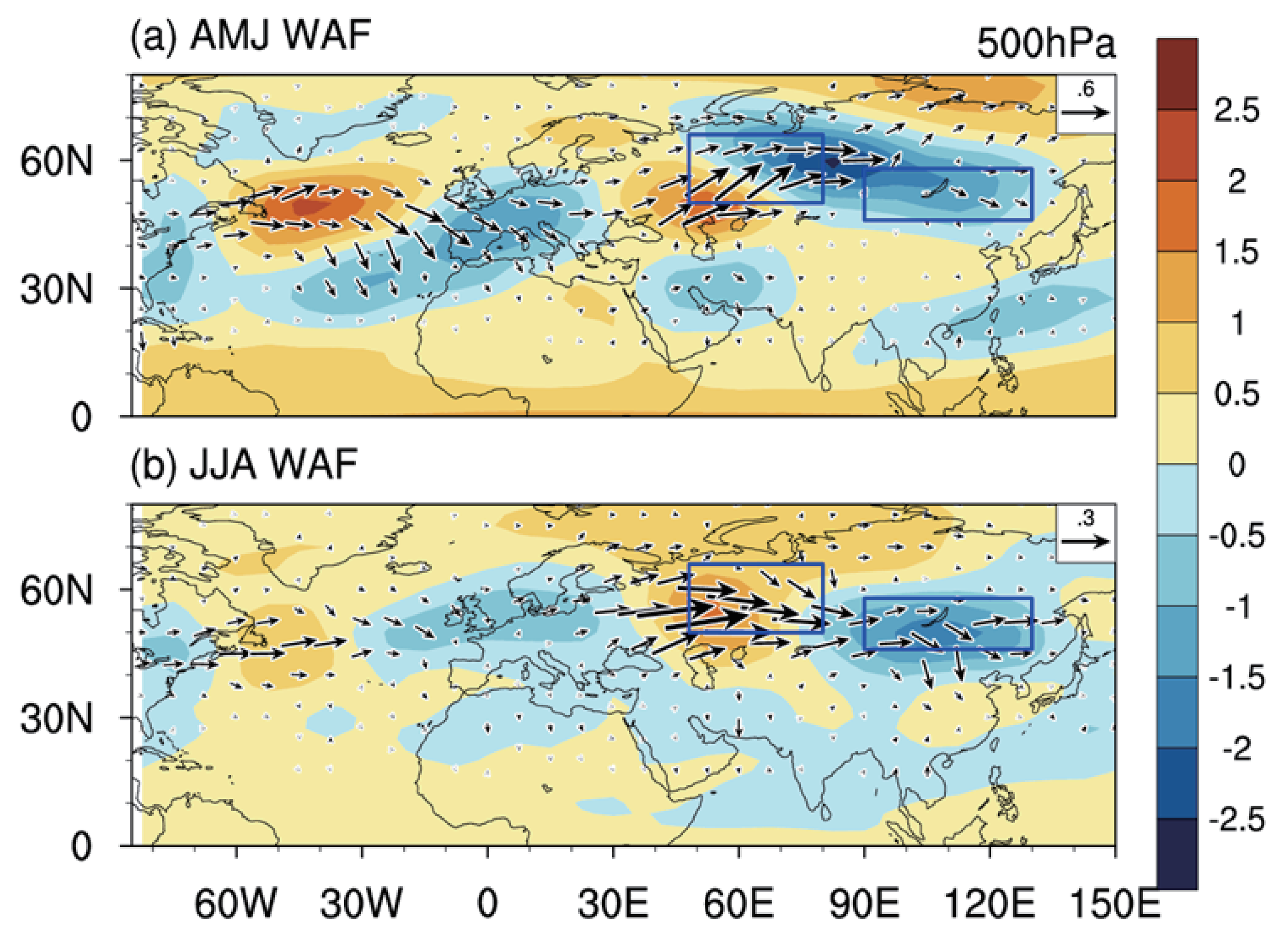

Figure 3. 500 hPa stream function (shading; units: m^2/s) and the associated wave activity flux (vector; units: m^2/s^2) anomalies regressed onto the SSDI index during (a) late spring (AMJ) and (b) summer (JJA). The rectangles are same as those in Figure 1.

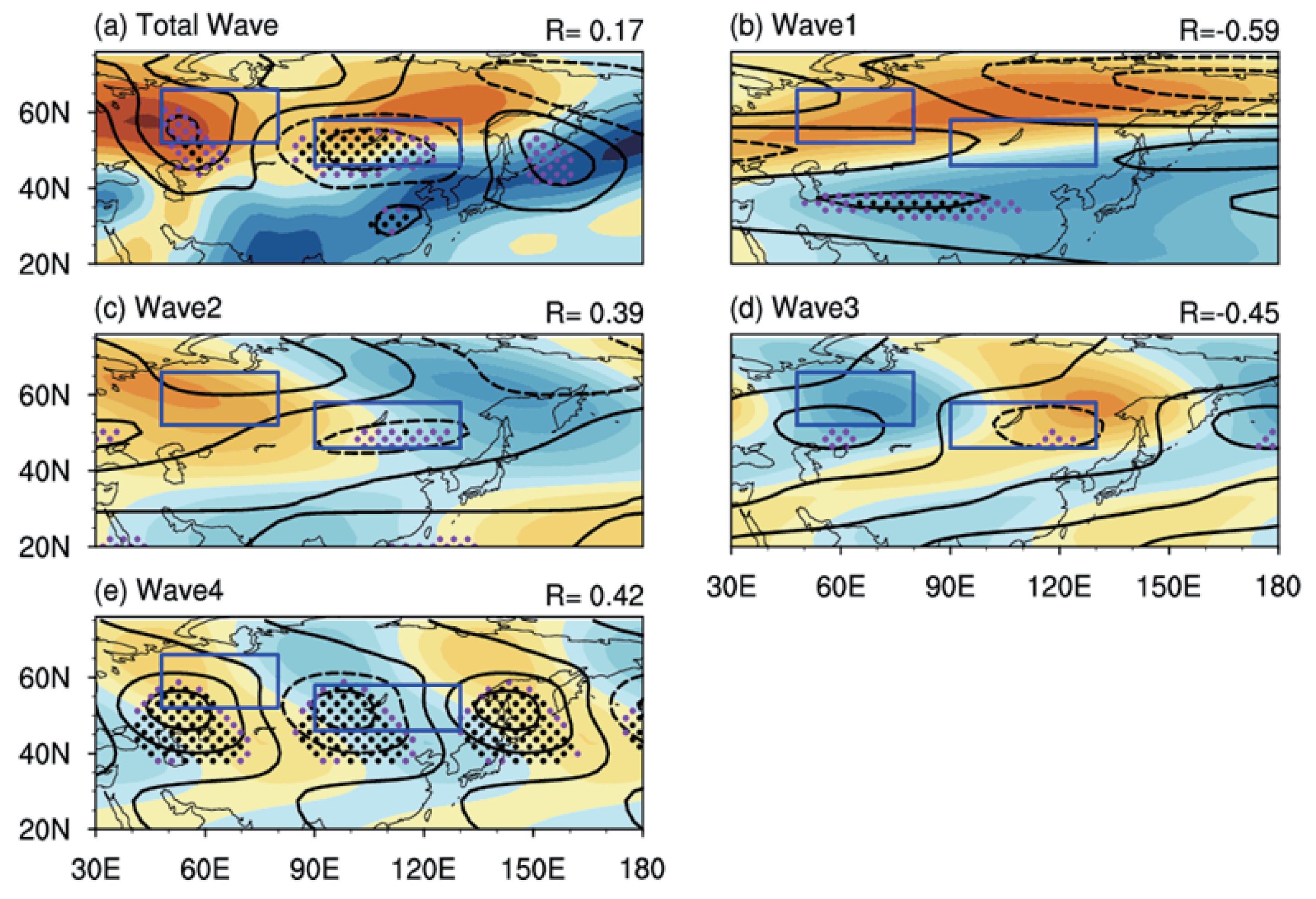

Figure 4. SSD forced (contours) and climatological (shading) stationary waves represented by summer 500 hPa geopotential heights for (a) total wave and (b–e) zonal wavenumbers 1–4. The stationary waves are obtained by removing the zonal mean of the geopotential heights. R denotes the spatial coefficients between the SSD forced and climatological waves. Contour intervals are 10 and 4 gpm for the climatological and SSD forced total waves, respectively, and 5 and 2 gpm for climatological and forced waves of zonal wavenumbers 1–4, respectively. The rectangles are same as those in Figure 1.